Published in final edited form as:
Science. 2010 June 4; 328(5983): 1281–1284. doi:10.1126/science.1188462.

FCHo Proteins are Nucleators of Clathrin-Mediated Endocytosis

William Mike Henne[1,2,*], **Emmanuel Boucrot**[1,*,†], **Michael Meinecke**[1], **Emma Evergren**[1], **Yvonne Vallis**[1], **Rohit Mittal**[1], and **Harvey T. McMahon**[1,†]

[1]MRC Laboratory of Molecular Biology, Hills Road, Cambridge, CB2 0QH, UK

Abstract

Clathrin-mediated endocytosis, the major pathway for ligand internalization into eukaryotic cells, is thought to be initiated by clustering of clathrin and adaptors around receptors destined for internalization. However, here we report that the membrane-sculpting F-BAR domain-containing FCHo1 and 2 (FCHo1/2) proteins were required for plasma membrane clathrin-coated vesicle (CCV) budding and marked sites of CCV formation. Changes in FCHo1/2 expression levels correlated directly with numbers of CCV budding events, ligand endocytosis, and synaptic vesicle marker recycling. FCHo1/2 proteins bound specifically to the plasma membrane and recruited the scaffold proteins, eps15 and intersectin, which in turn engaged the adaptor-complex AP2. The FCHo F-BAR membrane-bending activity was required, leading to the proposal that FCHo1/2 sculpt the initial bud site and recruit the clathrin machinery for CCV formation.

Clathrin-mediated endocytosis is the process by which cargo is internalized into vesicles with the aid of adaptors (like AP2) and the coat-protein clathrin (1, 2). Amphiphysins and sorting nexin 9 likely recruit the membrane scission protein dynamin to membranes of high curvature by their N-terminal BAR (Bin/Amphiphysin/Rvs) domains (3, 4). Here we investigate the possibility that membrane-sculpting proteins play an early role in invagination even prior to adaptor and clathrin recruitment. We studied the F-BAR-containing protein family FCHo1/2 (Fer/Cip4 homology domain only proteins 1 and 2) whose F-BAR homodimer module can recognize less extreme curvatures than BAR modules (5-7). FCHo1/2 are ubiquitously expressed (fig. S1A and B) and have a twisted shape distinct from the F-BAR dimers of FBP17 and CIP4 (5-7). The yeast homolog, Syp1, is recruited early to sites of actin-dependent endocytosis (8-10). We confirmed that FCHo1/2 are localized to clathrin-coated pits (CCPs) only on the plasma membrane (PM) (fig. S1C-F). Furthermore, an FCHo signal defined where a CCP forms, because it was detected before the visible appearance of clathrin or its PM specific adaptor, AP2 (Fig. 1A,C and fig. S2A-B). The FCHo1/2 signal decreased before the clathrin signal intensity reached its maximum but in some rare cases the FCHo protein did not leave, and defined sites where clathrin returned multiple times, thus marking endocytic ‘hot-spots’ (fig. S2C). FBP17, another F-BAR protein implicated in clathrin-mediated endocytosis (6) was, in contrast, recruited at later stages to some (3±1%) CCPs (fig. S2E). FCHo2 was detected by cryoimmuno-electron microscopy at early to late stages of CCPs consistent with live cell imaging kymographs

[†]To whom correspondence should be addressed: hmm@mrc-lmb.cam.ac.uk and eboucrot@mrc-lmb.cam.ac.uk.
[*]These authors contributed equally to this work.
[2]present address: Weill Institute for Cell and Molecular Biology, Cornell University, Ithaca, NY 14853, USA.

Supporting Online Material
www.sciencemag.org
Materials and Methods
Supporting Text
Figs. S1-S12
Movies S1, S2

Europe PMC Funders Author Manuscripts

(Fig. 1B). A complete loss of CCPs was observed when FCHo1+2 levels were greatly reduced using double RNAi (Fig. 1C-D and fig. S3A-D) with a concomitant reduction in internalization of three known cargoes for clathrin-mediated endocytosis: transferrin (Tf), low-density lipoprotein (LDL), and epidermal growth factor (EGF) (Fig. 1E). In the absence of FCHo proteins, both AP2 and clathrin were cytosolic. These phenotypes were rescued by an RNAi-resistant form of FCHo2 (Fig. 1C-E and fig. S3E) (11). FCHo1/2 function was not limited to fibroblasts but was also associated with clathrin-mediated endocytosis in primary astrocytes and recycling of synaptic vesicle markers (synaptotagmin1 and synaptophysin) following stimulated exocytosis in 4 DIV (days in vitro) hippocampal neurons (fig. S4). Overexpression of FCHo1 or FCHo2 led to a dramatic increase in CCP density. This increase wasnot due to slowed or inhibited CCV budding (as with epsin1 overexpression (fig. S5B) or dynamin inhibition by dynasore(12)) as CCPs were dynamic (increased nucleation rate) and functional (increased Tf uptake) during FCHo1/2 overexpression (Fig. 1F-H, fig. S5, Movie S1). Because CCP numbers directly correlate with FCHo1/2 levels, FCHo proteins appear to act as CCP nucleators.

The presence of a membrane bending protein early in CCP formation caused us to seek an explanation for how FCHo1/2 recruitment connects to clathrin recruitment. We looked for FCHo2 C-terminal AP2-μ homology domain (μHD) interactors in brain and HeLa cell extracts, and found that the main interaction partners were known CCP proteins eps15, eps15R and intersectin 1 and 2 (Fig. 2A and fig. S6A-B). The interaction of eps15 with the μHD was direct (fig. S6C and (8)) as was that with intersectin1. The CCP localization of eps15 and intersectin was dependent on FCHo1/2 (Fig. 2B). Notably, these proteins interact directly with AP2 but not with clathrin, unlike many other CCV accessory proteins (2). Eps15 and intersectin appearance coincided with that of FCHo2 (Fig. 2C), suggesting that these proteins constitute an early module for nascent CCP assembly. FCHo1/2 are necessary for CCP formation and yet their fluorescent intensity diminished before vesicle budding (Fig. 1A), just as dynamin intensity increased (fig. S6D). Similarly, the yeast Syp1 intensity decreased as Abp1 increased (9, 10). In purified CCVs, FCHo1/2, eps15 and intersectin levels were reduced compared to total extracts (Fig. 2D and fig. S6E), consistent with their absence in previous mass spectrometry studies (13). Thus, FCHo1/2 initiate CCPs but are excluded from mature vesicles, with FCHo1/2 being primarily PM-associated, consistent with their localization on constricted CCP necks (Fig. 2E).

RNAi of AP2 leads to a marked reduction in CCP numbers (14). Thus, we tested the localization of FCHo2 in the absence of AP2. While AP2 puncta were largely missing, FCHo2 puncta at the PM remained and still colocalized with eps15 and intersectin (Fig. 2G and fig. S7A). The FCHo2-μHD ligand interaction was also AP2-independent in vitro (Fig. 2F and fig. S7B). In contrast, the localization of epsin, another membrane sculpting molecule that binds clathrin and AP2, was dependent on the presence of AP2 (fig. S7C). An alternative strategy to disrupt CCP formation is the overexpression of the C-terminus of AP180, which binds to clathrin with high affinity (15). Overexpression led to an accumulation of AP2 puncta which co-localized with FCHo2, eps15 and intersectin but had no clathrin, and were static (fig. S7D-F). Thus FCHo2, eps15 and intersectin do not require AP2 or clathrin to cluster. An eps15/eps15R/intersectin1/intersectin2 quadruple knockdown affected FCHo2 clustering into puncta but not its PM localization, while AP2 was cytosolic (Fig. 2H and fig. S8A-E). RNAi of Dab2, a μHD interaction partner that arrives early at CCPs (fig. S6A and S8F) and that was not enriched in CCVs (Fig. 2D), did not lead to a reduction in CCPs (fig. S8F-G). Thus eps15 and intersectin cluster FCHo1/2 at nascent sites of CCP nucleation. Mutation of K797 in FCHo2 μHD (fig. S9A, a conserved residue that is equivalent to where AP2-β interacts with AP2-μ in pdb:2VGL) (16), abolished interactions with eps15 and intersectins (Fig. 2J and fig. S9B). In the FCHo1+2 RNAi background, K797E did not rescue CCP formation and Tf uptake, and was diffusely located on the PM

(Fig. 2I). Thus FCHo membrane recruitment and clustering by eps15 and intersectins initiates CCP maturation with subsequent recruitment of AP2 and clathrin leading to coated vesicle formation.

Functionality of F-BAR domains is mediated by three distinct properties: membrane binding, dimerization, and membrane sculpting (5, 6, 17). To test the importance of each property in FCHo2 function, we designed: i) a chimera replacing the F-BAR domain with a PM targeting PH domain, which dimerizes because of an EGFP tag (18), ii) a structure-based mutant of FCHo2 (F38E+W73E) which should disrupt dimer formation, and iii) a fluorescently-tagged SGIP1, a close relative of FCHo1/2 and a CCP component which has a C-terminal μHD but no F-BAR domain (19). All three proteins localized to CCPs in wild-type cells (fig. S10A), but upon depletion of endogenous FCHo1+2 did not rescue CCP formation (Fig 3A). As expected, both the PH chimera and SGIP1 localized to the PM (sometimes in large sheets) whereas the dimer mutant remained cytosolic. Thus, the dimeric, membrane sculpting F-BAR module is necessary for CCP formation. The region following the FCHo1/2 F-BAR domain (residues 263-430) is rich in positively charged amino acids and has a high homology with the N-terminus of SGIP1 (9). An extended F-BAR module containing this homology region (F-BAR-x for e**x**tended), showed enhanced membrane binding and tubulation in vitro (fig. S10B,C). The F-BAR-x module co-sedimented preferentially with liposomes enriched with $Pi(4,5)P_2$, helping to explain why FCHo proteins are PM targeted (Fig. 3B). Acute decrease of cellular $Pi(4,5)P_2$ levels by the addition of 1-butanol (20) led to acute relocalization of FCHo2 to the cytosol (fig. S10D), supporting the role of $Pi(4,5)P_2$ in the targeting of FCHo1/2 to the PM. The F-BAR-x module caused extensive tubulation of $Pi(4,5)P_2$-liposomes to high curvatures (from 130 to 18nm tubules and many small vesicles) in a protein concentration-dependent manner (Fig. 3C). Protein density surrounding tubules sometimes exhibited striations where the angle correlated with the degree of membrane curvature (fig. S10E and Movie S2). Narrower tubules displayed more oblique angles and the narrowest ones were twisted (Fig 3C) (5, 17). This provides a mechanistic explanation for the generation of increasing curvature required for CCP budding and dynamin recruitment. To test the contribution of membrane sculpting in FCHo2 function, we mutated two conserved lysines (K146E+K165E) on the concave face of the F-BAR module as well as a conserved residue (I268N) associated with a macrophage-induced autoimmune disease (21) and its interacting residue (L136E) along the F-BAR 'wing' (fig. S11A,B). As expected, the K146E+K165E mutant displayed reduced membrane binding in vitro and relocalized to the cytosol, whereas I268N and L136E mutations did not abrogate membrane binding but failed to tubulate the PM (fig. S11C,D). When placed into full-length FCHo2, I268N and L136E induced enlarged and static aberrant CCPs and could not rescue FCHo1+2 RNAi-induced Tf uptake defect (Fig. 3E). Thus FCHo2-mediated membrane sculpting is essential for normal CCP nucleation.

We showed that FCHo1/2 proteins nucleate CCPs and that AP2 is a later component recruiting clathrin, cargo and accessory proteins (fig. S12). We also uncovered a role for membrane sculpting in the initiation of clathrin-mediated endocytosis. Thus curvature generation appears to be fundamental to plasma membrane CCV formation from neurons to fibroblasts and FCHo 1 and 2 represent key initial proteins ultimately controlling cellular nutrient uptake, receptor regulation and synaptic vesicle retrieval.

Supplementary Material

Refer to Web version on PubMed Central for supplementary material.

Europe PMC Funders Author Manuscripts

Acknowledgments

We thank S.-Y. Peak-Chew for mass spectrometry, M. Daly for cell sorting, G. Lingley for movie design, J.E. Tyrrell for summer assistance and Perkin Elmer for support with spinning-disk microscopy. Support was provided to H.M.M. (Medical Research Council, UK), W.M.H. (LMB PhD Scholarship), E.B. (Human Frontiers Science Program Organization and MRC), M.M. and E.E. (EMBO fellowships).

References and Notes

1. Traub LM. Nat Rev Mol Cell Biol. 2009; 10:583. [PubMed: 19696796]
2. Schmid EM, McMahon HT. Nature. 2007; 448:883. [PubMed: 17713526]
3. Peter BJ, et al. Science. 2004; 303:495. [PubMed: 14645856]
4. Lundmark R, Carlsson SR. J Biol Chem. 2003; 278:46772. [PubMed: 12952949]
5. Henne WM, et al. Structure. 2007; 15:839. [PubMed: 17540576]
6. Shimada A, et al. Cell. 2007; 129:761. [PubMed: 17512409]
7. http://www.endocytosis.org/F-BAR_proteins/BAR-Comparisons.html
8. Reider A, et al. Embo J. 2009; 28:3103. [PubMed: 19713939]
9. Stimpson HE, Toret CP, Cheng AT, Pauly BS, Drubin DG. Mol Biol Cell. 2009; 20:4640. [PubMed: 19776351]
10. Boettner DR, et al. Curr Biol. 2009; 19:1979. [PubMed: 19962315]
11. Materials and methods are available as supporting material on Science Online.
12. Macia E, et al. Dev Cell. 2006; 10:839. [PubMed: 16740485]
13. Blondeau F, et al. Proc Natl Acad Sci U S A. 2004; 101:3833. [PubMed: 15007177]
14. Motley A, Bright NA, Seaman MN, Robinson MS. J Cell Biol. 2003; 162:909. [PubMed: 12952941]
15. Ford MG, et al. Science. 2001; 291:1051. [PubMed: 11161218]
16. Collins BM, McCoy AJ, Kent HM, Evans PR, Owen DJ. Cell. 2002; 109:523. [PubMed: 12086608]
17. Frost A, et al. Cell. 2008; 132:807. [PubMed: 18329367]
18. Zacharias DA, Violin JD, Newton AC, Tsien RY. Science. 2002; 296:913. [PubMed: 11988576]
19. Uezu A, et al. J Biol Chem. 2007; 282:26481. [PubMed: 17626015]
20. Boucrot E, Saffarian S, Massol R, Kirchhausen T, Ehrlich M. Exp Cell Res. 2006; 312:4036. [PubMed: 17097636]
21. Grosse J, et al. Blood. 2006; 107:3350. [PubMed: 16397132]

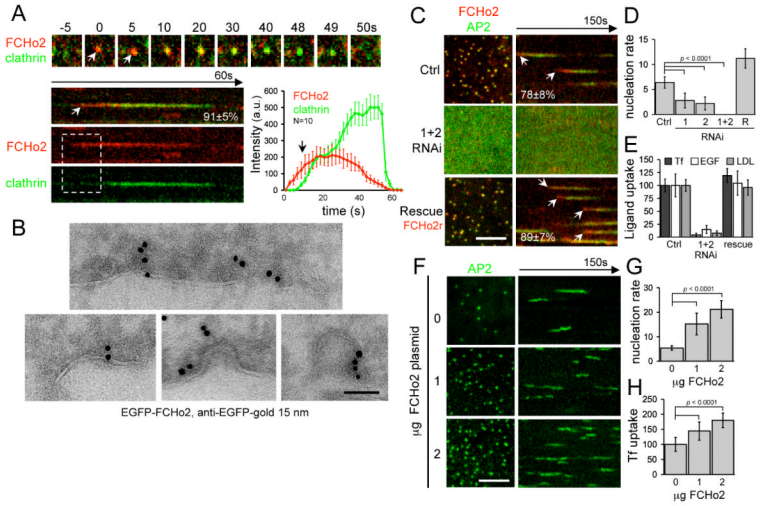

Fig. 1.

FCHo1/2 proteins are clathrin/AP2 nucleators. (**A**) Dynamic cell surface localization (top) and kymograph (bottom) of representative CCPs labelled with RFP-FCHo2 (FCHo2) and GFP-LCa (clathrin). FCHo2 was detected before clathrin (white arrows and graph). a.u.: arbitary units. (**B**) Cryoimmuno-electron microscopy localized GFP-FCHo2 at CCPs. Scale bar 100nm. (**C**) CCVs, labelled by σ2-GFP (AP2), did not form with double RNAi of FCHo1+2 (FCHo1+2 RNAi) where AP2 became cytosolic (contrast enhanced to show the diffuse signal at the plasma membrane). Inhibition was relieved by co-expression of RNAi-resistant RFP-FCHo2 (rescue). (**D**) Nucleation rates (number of new CCPs/10^4µm^2/second) in cells treated with scrambled RNAi (Ctrl), RNAi against FCHo1 (1), FCHo2 (2), FCHo1+2 (1+2) or rescue (R). (**E**) Clathrin ligands, transferrin (Tf) epidermal growth factor (EGF) and low-density lipoprotein (LDL) uptake in cells treated as in C. (**F**) Clathrin vesicles (AP2) in BSC1 cells transfected with 0, 1 or 2µg of untagged-FCHo2 for 2×10^5 cells. (**G**) Nucleation rate and (**H**) Tf uptake in cells treated as in F. Scale bars, 5µm (C,F) and 200nm (B). Displayed kymographs were representative (percentage, n=319 CCPs (11)).

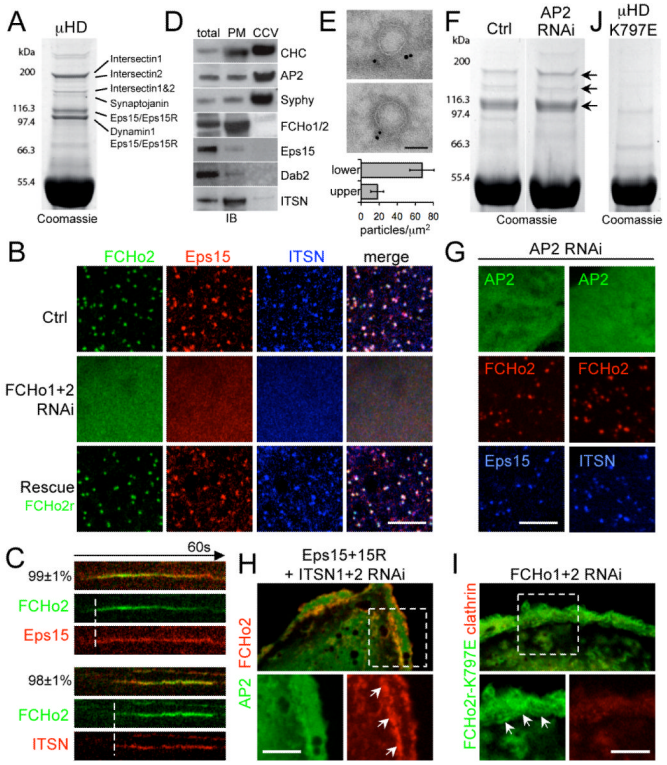

Fig. 2.

FCHo2 directly binds and recruits eps15 and intersectin to initiate CCP maturation. (**A**) Pull down with GST-FCHo2-μHD and rat brain lysate. Interacting proteins were identified by mass spectrometry. (**B**) Eps15 and intersectin (ITSN) formed puncta at the PM colocalizing with FCHo2. In double FCHo1+2 RNAi cells, Eps15 and ITSN were cytosolic (contrast enhanced to show the diffuse signal); co-expression of RNAi-resistant FCHo2 (FCHo2r) rescued PM-targeting (Rescue). (**C**) Kymograph of representative CCPs (percentage, (11)) labeled with FCHo2 and Eps15 or ITSN. (**D**) FCHo2, eps15, and ITSN were CCV de-enriched. Clathrin (CHC), AP2, and vesicle marker synaptophysin (Syphy) displayed enrichment in CCV fractions (CCV). FCHo2 and ITSN were PM enriched. IB: immunoblot. (**E**) Cryoimmuno-electron microscopy of GFP-FCHo2 localized it to the CCP neck. Bar graph shows gold particle density in the upper and lower half of constricted CCPs ($p<0.01$). (**F**) Pull downs with GST-μHD from scrambled (left) or AP2 RNAi (right) treated HeLa cells. Eps15 and ITSN bands were visible in both (arrows). (**G**) Upon AP2 depletion (μ2 RNAi) σ2-GFP (another AP2 subunit) was cytosolic (contrast enhanced to show the diffuse signal), but Eps15 and ITSN still co-localize with FCHo2 at the PM (arrows). (**H**) FCHo2 and AP2 (σ2-GFP) puncta disappeared under Eps15 + Eps15R + ITSN1 + ITSN2 quadruple RNAi. AP2 became cytosolic (diffuse signal) whereas FCHo2 remained at the PM (inset). (**I**) In FCHo1+2 RNAi cells, RNAi-resistant FCHo2-K797E (FCHo2r-K797E) bound to the PM (arrows) but did not cluster nor rescue CCP formation, reported by RFP-LCa (clathrin). In these cells FCHo1+2 RNAi inhibition of Tf uptake was also not rescued (7.2±3.5% of control uptake ($p<0.0001$). (**J**) GST-μHD K797E no longer pulled-down the protein bands visible in A. Green, red and blue panels indicate GFP-, RFP-, and BFP-tagged proteins respectively. Scale bars, 5μm. (B,H,G,I) and 100nm (E).

Europe PMC Funders Author Manuscripts

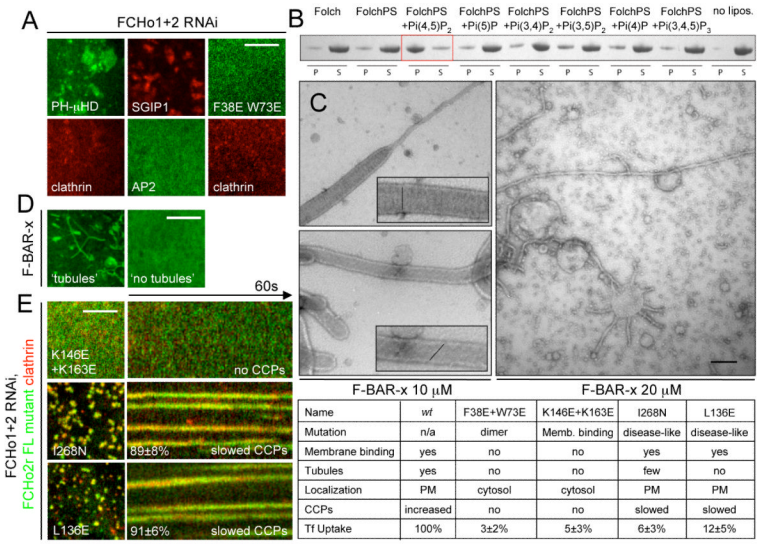

Name	wt	F38E+W73E	K146E+K163E	I268N	L136E
Mutation	n/a	dimer	Memb. binding	disease-like	disease-like
Membrane binding	yes	no	no	yes	yes
Tubules	yes	no	no	few	no
Localization	PM	cytosol	cytosol	PM	PM
CCPs	increased	no	no	slowed	slowed
Tf Uptake	100%	3±2%	5±3%	6±3%	12±5%

Fig. 3.

Lipid binding and membrane sculpting FCHo1/2 abilities are both essential for CCP formation. (**A**) Chimeric GFP-PLC-PH+FCHo2μHD (PH-μHD), a dimer interface mutant GFP-FCHo2(F38E+W73E), and RFP-SGIP1 all could not rescue CCP nucleation - monitored by following either clathrin or AP2 fluorescence - in double RNAi FCHo1+2 cells. (**B**) Lipid co-sedimentation assay of 15μM F-BAR-x in presence of 1mg/mL liposomes: Folch (Avanti brain lipid), FolchPS (80% Folch, 20% phosphatidylserine) or FolchPS +5% of indicated PiPs. Liposome-bound proteins were pelleted (P) by ultracentrifugation, unbound protein remained in the supernatant (S). (**C**) Folch+15%PS +5%Pi(4,5)P_2 liposomes incubated with either 10 or 20μM F-BAR-x and spotted onto EM grids gave mainly tubules of diameters of 50-80nm (10 μM) or 18nm (20μM, most were visibly twisted). Insets show enlargements with protein density striations. (**D**) F-BAR-x-induced in vivo tubulation: representative images of 'tubules' and 'no tubules'. (**E**) RNAi-resistant form of full-length FCHo2 (FCHo2r) with membrane-binding mutation (K146E +K163E) remained cyosolic and could not rescue FCHo1/2 RNAi-mediated absence of CCPs, whereas FCHo2r containing membrane-sculpting mutations (I268N and L136E) displayed slowed and aberrant CCPs. Displayed kymographs were representative (percentage, (11)). Table summarizing the mutants and their phenotypes. Scale bars, 5μm (A,D,E) and 100nm (C).